Klein Backscattering and Fabry-Pérot Interference in Graphene Heterojunctions

Andrei V. Shytov,[1] Mark S. Rudner,[2] and Leonid S. Levitov[2]

[1]*Department of Physics, University of Utah, Salt Lake City, Utah 84112, USA*
[2]*Department of Physics, Massachusetts Institute of Technology, Cambridge, Massachusetts 02139, USA*

We present a theory of quantum-coherent transport through a lateral *p-n-p* structure in graphene, which fully accounts for the interference of forward and backward scattering on the *p-n* interfaces. The backreflection amplitude changes sign at zero incidence angle because of the Klein phenomenon, adding a phase π to the interference fringes. The contributions of the two *p-n* interfaces to the phase of the interference cancel with each other at zero magnetic field, but become imbalanced at a finite field. The resulting half-period shift in the Fabry-Pérot fringe pattern, induced by a relatively weak magnetic field, can provide a clear signature of Klein scattering in graphene. This effect is shown to be robust in the presence of spatially inhomogeneous potential of moderate strength.

The electron system in graphene features surprising connections with the relativistic quantum mechanics of a massless Dirac particle in external electric and magnetic fields [1–5]. In particular, charge flow in lateral *p-n* junctions in graphene is described by Klein scattering [3,4,6], exhibiting perfect transmission through the barrier at normal incidence, regardless of the barrier characteristics, and a barrier-dependent, finite reflection coefficient at nonnormal incidence [7]. On the experimental side, while transport properties of the first *p-n* junctions fabricated in graphene were dominated by disorder [8–10], two recent papers [11,12] report on observations of a contribution to the conductance consistent with expectations for ballistic transmission through *p-n* interfaces. To extract this "intrinsic" contribution, which is relatively small in magnitude, one must account for the screening of the gate potential [13] and the effects of disorder [14].

What other features, besides collimated transmission, may serve as an experimental signature of Klein scattering? Here we focus on the characteristic behavior of the reflection amplitude, which exhibits a jump in phase by π when the incidence angle α is varied from positive to negative values (see Fig. 1). The sign change occurs at normal incidence because the reflection amplitude vanishes at $\alpha = 0$. Below we show that this phase shift, which is fundamental to Klein scattering, could serve as a hallmark of Klein physics in graphene.

The backreflection phase can be detected from interference of electron waves scattered on two parallel *p-n* boundaries in a *p-n-p* structure. Transmission in this system, described by the Fabry-Pérot (FP) model, exhibits periodic dependence on the phase $\Delta\theta$ gained by an electron bouncing between the *p-n* interfaces (see Fig. 1),

$$\Delta\theta = 2\theta_{\mathrm{WKB}} + \Delta\theta_1 + \Delta\theta_2, \qquad (1)$$

where $\theta_{\mathrm{WKB}} = \frac{1}{\hbar}\int_1^2 p_x(x')dx'$ is the WKB phase and $\Delta\theta_{1(2)}$ are the backreflection phases for the interfaces 1 and 2, exhibiting a π-jump at zero incidence angle α.

As illustrated in Fig. 1, the contribution $\Delta\theta_1 + \Delta\theta_2$ to the net phase can be altered by a magnetic field. At zero B the incidence angles at interfaces 1 and 2 have opposite signs, and thus the jumps in $\Delta\theta_{1(2)}$ cancel. However, for curved electron trajectories at a finite B, the signs of the incidence angles can be made equal. Indeed, because of translational invariance along the *p-n* interface, in the presence of a magnetic field the y component of electron kinetic momentum varies in space as $\tilde{p}_y(x) = p_y - eBx$, where p_y is the conserved canonical momentum component that labels different trajectories. For the incidence angles at interfaces 1 and 2 to be of equal sign, $\tilde{p}_y(x_1)$ and $\tilde{p}_y(x_2)$ must have opposite signs, which happens when

$$-eBL/2 < p_y < eBL/2. \qquad (2)$$

In this case the net backreflection phase $\Delta\theta_1 + \Delta\theta_2$ in (1) equals π. As we shall see, the backreflection phase manifests itself as *half a period shift* of the FP fringe contrast. This phase shift develops for the field strength such that the
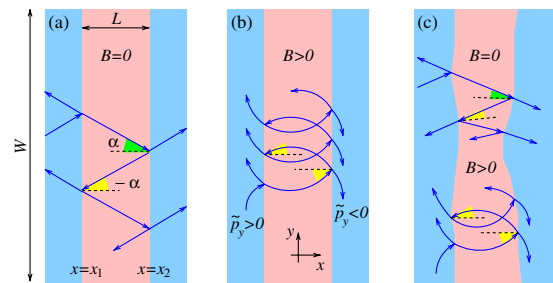

FIG. 1 (color online). Schematic of electron transmission through a *p-n-p* structure at zero (a) and finite (b) magnetic field *B*. The amplitude of backreflection changes sign at the incidence angle $\alpha = 0$. At finite *B*, the angles of incidence on both *p-n* interfaces are of the same sign for the trajectories satisfying condition (2). This adds a phase of π to the electron phase accumulated between reflections, resulting in a half-period shift of Fabry-Pérot interference fringes. (c) Weak spatial inhomogeneity does not alter the relative sign of incidence angles.

range (2) exceeds the Klein collimation range in which the p-n interface is transparent.

One useful feature of the jump in backreflection phase is that it is less momentum-selective than collimated transmission. A potential difficulty, however, is that the interference of scattering on two p-n interfaces can be sensitive to disorder. Below we will investigate the dependence of the FP contrast on magnetic field in the presence of large-scale spatial fluctuations. We find that, while the FP fringe contrast is suppressed, the $1/2$-period shift, controlled by backreflection, remains surprisingly robust. Even at a relatively high disorder strength, when the FP contrast is strongly reduced and the fringes become aperiodic, the $1/2$-period shift induced by the magnetic field remains clearly discernable.

Here we shall model the gate potential by a parabola $U(x) = ax^2 - \varepsilon$, which at $\varepsilon > 0$ creates p-n interfaces at

$$x = \pm x_\varepsilon, \qquad x_\varepsilon \equiv \sqrt{\varepsilon/a}. \qquad (3)$$

The potential depth is controlled by a top gate, $\varepsilon = \beta V_{tg}$ (in Ref. [11], $\beta \approx \frac{1}{300}$). The curvature parameter a is determined by the width of the top gate L_{tg} and its height h above the graphene plane. The actual potential profile may be nonparabolic (see Ref. [11] for modeling of screening effects), however this difference should not matter for FP interference, occurring when the separation between p-n interfaces $L = 2x_\varepsilon$ spans only few de Broglie wavelengths. This is the case near the threshold in V_{tg} at which the p-n-p structure forms, where L is small compared to h and L_{tg}. The parabolic $U(x)$ may also provide a reasonable approximation for the devices described in Ref. [12], especially those with narrow top gates.

The Hamiltonian for a two-component Dirac wave function, in the presence of the potential $U(x)$, is

$$\mathcal{H} = v_F \sigma_3 p_x + v_F \sigma_2 (p_y - eBx) + U(x) \qquad (4)$$

where $\sigma_{2,3}$ are Pauli matrices, $v_F \approx 1.1 \times 10^6$m/s is the Fermi velocity in graphene, and B is the magnetic field. Hereafter we set $\hbar = v_F = 1$, with the units for energy, length and magnetic field as follows:

$$\varepsilon_* = (av_F^2\hbar^2)^{1/3} \approx 14 \text{ meV}, \qquad x_* = \hbar v_F/\varepsilon_* \approx 53 \text{ nm},$$

$$B_* = \Phi_0/2\pi x_*^2 \approx 0.24 \text{ T}, \qquad (\Phi_0 = h/e), \qquad (5)$$

where we used the curvature a of 5 eV$/\mu$m^2, obtained from the model potential of Ref. [11] fitted to a parabola. Because of the weak $a^{1/3}$ dependence, the estimates (5) should also apply, at least roughly, to other systems.

To find the transmission and reflection coefficients, we factorize the wave function as $\psi(x, y) = e^{ip_y y}\psi(x)$, and solve the one-dimensional Schrödinger equation

$$i\partial_x \psi = (U(x)\sigma_3 - i(p_y - eBx)\sigma_1)\psi, \qquad (6)$$

where without loss of generality we set the Fermi energy equal to zero. Transmission, evaluated from the numerical solution of Eq. (6), exhibits resonances as a function of

momentum and potential depth, shown in Fig. 2. We note a drastic difference between the results at zero B, similar to those of Refs. [15,16], and the results at finite B.

To understand the behavior of transmission, it is instructive to view the differential equation (6) as a fictitious time-dependent Schrödinger evolution of a two-level system, the coordinate x playing the role of time. In this analogy, the system is driven through an avoided level crossing with splitting $-2i(p_y - eBx)$ at the crossing times determined by degeneracy of the diabatic states, $U(x) = ax^2 - \varepsilon = 0$. This condition yields $x = \pm x_\varepsilon$, Eq. (3). A Landau-Zener transition at the first level crossing creates a coherent superposition of the diabatic states that can interfere at the second crossing. This so-called Stückelberg interference (see [17] and references therein), which can be constructive or destructive, is described by an oscillatory function of the phase $\Delta\theta = -2\int_{-x_\varepsilon}^{x_\varepsilon} U(x)dx = \frac{4}{3}\varepsilon x_\varepsilon$ gained between the crossings. The locations of interference fringes, determined from the conditions $\Delta\theta = 2\pi n$ with $n = 1, 2\ldots$, are $\varepsilon_n = (3\pi n/2)^{2/3}\varepsilon_*$, which agrees with the positions of the fringes seen in Fig. 2.

For $B = 0$, the suppression of oscillations near zero p_y can be linked to the absence of Landau-Zener transitions at vanishing level splitting. In the scattering picture, this is nothing else than the Klein phenomenon of perfect transmission at normal incidence. At finite B, the oscillations
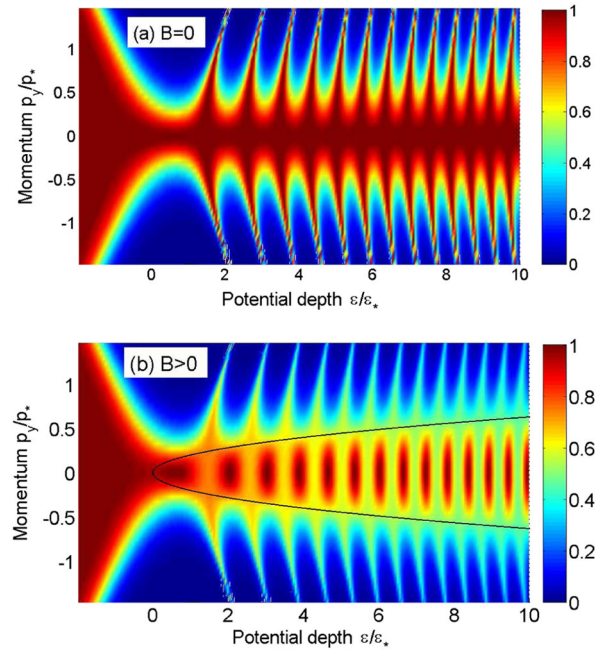

FIG. 2 (color online).   Transmission of the p-n-p structure (a) at zero magnetic field and (b) at a finite field of $B = 0.2\Phi_0/x_*^2$. Electron momentum p_y is measured in units of $p_* = v_F/\varepsilon_*$. Note that at finite B the fringe contrast is reversed across the parabola (7) (black line), with the maxima and minima of the fringe pattern interchanging. This behavior is in agreement with the Fabry-Pérot model (9), with the reflection amplitude vanishing on the parabola, and changing its sign.

disappear when one of the level splittings $p_y \pm eBx_\varepsilon$ vanishes, suppressing one of the Landau-Zener transitions. In terms of electron motion, this condition is equivalent to the requirement of normal incidence on either of the interfaces (3), giving

$$p_y = \pm eB\sqrt{\varepsilon/a}, \qquad (7)$$

which is the black parabola drawn in Fig. 2(b). Indeed, fringes disappear on this line; upon crossing the line, the maxima and minima of fringes interchange, indicating a π phase shift in the phase of fringe contrast.

A more refined description can be obtained from a quasiclassical solution [15] with position-dependent momentum $p_x(x) = \sqrt{U^2(x) - \tilde{p}_y^2(x)}$. The turning points, defined by $p_x = 0$, are arranged as $x_{1'} < x_1 < x_2 < x_{2'}$, with x_2 and $x_{2'}$ equal to

$$\sqrt{\varepsilon + b^2 - p_y} + b, \qquad \sqrt{\varepsilon + b^2 + p_y} - b, \qquad (8)$$

where $b = \frac{1}{2}eB$ and $x_{1(1')}(p_y) = -x_{2(2')}(-p_y)$. Hereafter we set $a = 1$, restoring physical units later. Remarkably, the conditions $x_1 = x_{1'}$ and $x_2 = x_{2'}$, which correspond to one of the p-n interfaces becoming transparent because of the Klein phenomenon, yield a relation between p_y and ε which is identical to Eq. (7) found above.

The classically forbidden regions $x_{1'} < x < x_1$ and $x_2 < x < x_{2'}$, where p_x is imaginary, correspond to the Klein barriers at the interfaces 1 and 2. Denoting the corresponding transmission coefficients as t_1 and t_2, we can write the net transmission of the entire p-n-p structure in a general Fabry-Pérot form

$$T(p_y) = \frac{t_1 t_2}{|1 - \sqrt{r_1 r_2}e^{i\Delta\theta}|^2}, \qquad (9)$$

where $r_{1(2)} = 1 - t_{1(2)}$ are the reflection coefficients, and the phase $\Delta\theta$ is a sum of the WKB part and the phases of the reflection amplitudes, Eq. (1).

The transmission amplitudes $t_{1(2)}$ can be evaluated in the WKB tunneling approximation:

$$t_1 = e^{-2\mathrm{Im}\int_{x_1}^{x_{1'}} p_x(x')dx'} \approx e^{-\lambda(p_y - eBx_\varepsilon)^2}, \qquad \lambda = \frac{\pi}{2ax_\varepsilon}, \qquad (10)$$

with the integral computed by linearizing $U(x)$ near $x = x_\varepsilon$. Similarly, linearizing $U(x)$ near $x = -x_\varepsilon$, we find $t_2 = e^{-\lambda(p_y + eBx_\varepsilon)^2}$. Thus, the reflection amplitudes are

$$\mathrm{sgn}\,(p_y \pm eBx_\varepsilon)e^{i\theta_{\mathrm{reg}}(p_y)}\sqrt{1 - e^{-\lambda(p_y \pm eBx_\varepsilon)^2}}, \qquad (11)$$

where we factored the sign, responsible for the phase jump, and a regular part of the phase $e^{i\theta_{\mathrm{reg}}}$, as follows from analyticity in p_y. Because the WKB treatment is exact for linear potentials [18], and the transmission (10) is exponentially small unless $|p_y \pm eBx_\varepsilon| \lesssim \lambda^{-1/2}$, the linearization of $U(x)$ used to evaluate the integral in (10) gives accurate results for the energies of interest, $\varepsilon \gtrsim \varepsilon_*$.

The dispersion of the resonances in Fig. 2 can be understood from the momentum dependence of the quasiclassical WKB phase (for simplicity, we set $B = 0$):

$$\theta_{\mathrm{WKB}} = \int_{x_1}^{x_2} p_x(x')dx' \approx \frac{4}{3}\varepsilon^{3/2} - \frac{p_y^2}{2\varepsilon^{1/2}}\log\frac{\varepsilon}{|p_y|}, \qquad (12)$$

where an expansion in the parameter $|p_y/\varepsilon| \ll 1$ is legitimate because Klein collimation restricts transmission to $\Delta p_y \sim \lambda^{-1/2}$. The quantization condition $\theta_{12} = \pi(n + \frac{1}{2})$ gives the resonance energies $\varepsilon_n(p_y)$ dispersing as in Fig. 2.

To summarize, the FP model (9) is in full agreement with our numerical results. In particular, it explains the striking difference between the behavior at zero and finite B, as well as the phase shift of the fringe pattern, resulting from a sign change of the reflection amplitudes, Eq. (11).

These results can now be applied to analyze conductance and resistance, given by

$$R = G^{-1}, \qquad G = \frac{4e^2}{h}W\int_{-\infty}^{\infty} T(p_y)\frac{dp_y}{2\pi}, \qquad (13)$$

where W is the width of the p-n-p structure (see Fig. 1). As illustrated in Fig. 3, the resistance exhibits fringes which obey the $n^{2/3}$ scaling, as expected from the phase dependence on ε, Eq. (12). Somewhat surprisingly, the integral over p_y in (13) yields a fairly high fringe contrast in R. This results from the fact that Klein collimation effectively restricts the integral to the range of p_y where the resonances, Eq. (12), are nondispersing.

In the presence of the magnetic field, alongside with the overall increase in resistance, we observe that the fringes shift up in ε by approximately half a period (see Fig. 4). This shift, which is a direct consequence of the π-shift of the reflection phase discussed above, fully develops in the fields $B \sim 0.4B_*$. For the parameter values used above, Eq. (5), we find a value of about 0.1 T, which is well below the fields characteristic for magnetoresistance [11,12].
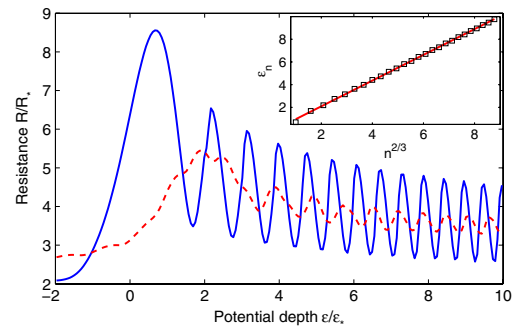

FIG. 3 (color online). Fringes in resistance (13) at $B = 0$, plotted in the units of $R_* = (x_*/W)h/4e^2$ (blue line). Inset illustrates a $n^{2/3}$ scaling for the maxima and minima of R, which is consistent with the $\varepsilon^{3/2}$ dependence of the WKB phase (12). Averaging over smooth potential fluctuations, described by a sum of a few harmonics, suppresses fringe contrast (red dashed line). Here we use Eq. (14) with $\sum_m |a_m| = 3\varepsilon_*$.
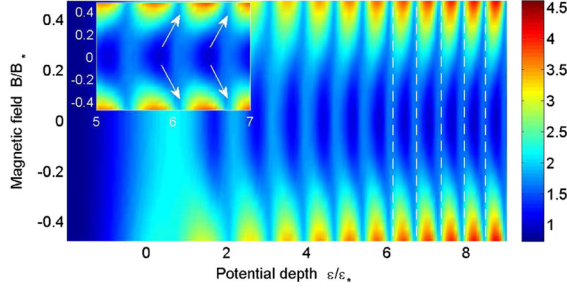
FIG. 4 (color online). Resistance (13) of the p-n-p structure as a function of magnetic field and potential depth. The quantity plotted is $\log R/R_*$, with $R_* = (x_*/W)h/4e^2$. The resistance minima at high B, marked by dashed lines, are shifted by approximately half a period relative to those at zero B. In the close-up of a few fringes (inset), arrows indicate the field-induced shift.

The effect of large-scale potential fluctuations, either intrinsic [19] or induced by variable distance to gates, can be analyzed by averaging the conductance in (13) over random offsets in potential depth ε:

$$\langle G \rangle = \oint G\Big(\varepsilon - \sum_m a_m \cos(m\phi + \phi_m)\Big)\frac{d\phi}{2\pi}. \qquad (14)$$

This simple model describes a smooth inhomogeneity with correlation length larger than the p-n interface separation L, but much shorter than the structure width W. The averaging procedure (14), applied to our numerical results, makes the fringes aperiodic and suppresses the contrast (see red dashed line in Fig. 3). However, the π phase shift induced by magnetic field remains clearly discernible even for relatively strong fluctuations [20].

At even stronger randomness, the FP transmission (9) can be replaced by its phase-averaged value

$$\langle T \rangle_\theta = \frac{t_1 t_2}{1 - r_1 r_2} = \frac{1}{e^{\lambda(p_y + eBx_\varepsilon)^2} + e^{\lambda(p_y - eBx_\varepsilon)^2} - 1}. \qquad (15)$$

Plugged in (13), it yields magnetoresistance with characteristic $B \sim B_*$, identical to that discussed in [4]. The resulting exponential suppression of conductance of course would hold only in the absence of short-range disorder.

Conspicuously, the resistance data [11,12] feature aperiodic oscillations in gate voltage, observed above the point where the sign of carriers beneath the top gate is reversed. This is the same region where strong FP fringes are expected for an ideal system. The energy scale of the oscillations reported in Ref. [11], converted from gate voltage using $\delta\varepsilon/\delta V_{\rm tg} \approx \frac{1}{300}$, is about $\delta\varepsilon \sim 30$ mV, which is only a few times larger than the period of $0.8\varepsilon_* \approx 11$ mV found above (Figs. 3 and 4). Could these oscillations, or those seen in [12], be the FP fringes contaminated by disorder? Comparison to the behavior of the FP contrast in the presence of magnetic field, in particular, to the π phase shift (Fig. 4), may help to clarify this.

In summary, Fabry-Pérot interference in the Klein scattering regime is found to be sensitive to the phase of the reflection amplitude that exhibits a jump by π near zero incidence angle. This leads to half a period shift of interference fringes in the presence of a relatively weak magnetic field, a new effect that can help to identify the Klein phenomenon in graphene.

Note added.—Recently, we became aware of the work [21] which reports unambiguous FP oscillations in a p-n-p structure. At low fields $B \lesssim 1$ T the behavior of the observed fringes is consistent with our predictions, however at higher fields the fringes are found to continuously transform into Shubnikov-deHaas oscillations instead of being suppressed. This indicates coexistence of momentum conserving and impurity assisted contributions to transport, which are dominant at low and high B, respectively. The FP and SdH oscillations can be understood on equal footing from quantization of periodic orbits of an electron bouncing between p-n boundaries (to be published).

[1] V. P. Gusynin and S. G. Sharapov, Phys. Rev. Lett. **95**, 146801 (2005).
[2] N. M. R. Peres, F. Guinea, and A. H. Castro Neto, Phys. Rev. B **73**, 125411 (2006).
[3] M. I. Katsnelson, K. S. Novoselov, and A. K. Geim, Nature Phys. **2**, 620 (2006).
[4] V. V. Cheianov and V. I. Falko, Phys. Rev. B **74**, 041403 (2006).
[5] A. V. Shytov, M. I. Katsnelson, and L. S. Levitov, Phys. Rev. Lett. **99**, 236801 (2007); Phys. Rev. Lett. **99**, 246802 (2007).
[6] C. W. J. Beenakker, arXiv:0710.3848.
[7] O. Klein, Z. Phys. **53**, 157 (1929).
[8] B. Huard *et al.*, Phys. Rev. Lett. **98**, 236803 (2007).
[9] J. R. Williams, L. C. DiCarlo, and C. M. Marcus, Science **317**, 638 (2007).
[10] B. Özyilmaz *et al.*, Phys. Rev. Lett. **99**, 166804 (2007).
[11] R. V. Gorbachev, A. S. Mayorov, A. K. Savchenko, D. W. Horsell, and F. Guinea, Nano Lett. **8**, 1995 (2008).
[12] N. Stander, B. Huard, and D. Goldhaber-Gordon, arXiv:0806.2319.
[13] L. M. Zhang and M. M. Fogler, Phys. Rev. Lett. **100**, 116804 (2008).
[14] M. M. Fogler, L. I. Glazman, D. S. Novikov, and B. I. Shklovskii, Phys. Rev. B **77**, 075420 (2008).
[15] P. G. Silvestrov and K. B. Efetov, Phys. Rev. Lett. **98**, 016802 (2007).
[16] J. M. Pereira, P. Vasilopoulos, and F. M. Peeters, Appl. Phys. Lett. **90**, 132122 (2007).
[17] D. M. Berns *et al.*, Nature (London) **455**, 51 (2008).
[18] A. V. Shytov, Nan Gu, and L. S. Levitov, arXiv:0708.3081.
[19] J. Martin *et al.*, Nature Phys. **4**, 144 (2008).
[20] See Fig. 4b and accompanying discussion in: A. V. Shytov, M. S. Rudner, and L. S. Levitov, arXiv:0808.0488.
[21] A. F. Young and P. Kim, arXiv:0808.0855.